Dilatancy in the Fracture of Crystalline Rocks

W. F. BRACE

U. S. Geological Survey and Department of Geology and Geophysics
Massachusetts Institute of Technology, Cambridge

B. W. PAULDING, JR.[1]

Illinois Institute of Technology Research Institute, Chicago

C. SCHOLZ

Department of Geology and Geophysics
Massachusetts Institute of Technology, Cambridge

Volume changes of a granite, a marble, and an aplite were measured during deformation in triaxial compression at confining pressure of as much as 8 kb. Stress-volumetric strain behavior is qualitatively the same for these rocks and a wide variety of other rocks and concrete studied elsewhere. Volume changes are purely elastic at low stress. As the maximum stress becomes one-third to two-thirds the fracture stress at a given pressure, the rocks become dilatant; that is, volume increases relative to elastic changes. The magnitude of the dilatancy, with a few exceptions, ranges from 0.2 to 2.0 times the elastic volume changes that would have occurred were the rock simply elastic. The magnitude of the dilatancy is not markedly affected by pressure, for the range of conditions studied here.

For granite, the stress at which dilatancy was first detected was strongly time dependent; the higher the loading rate the higher the stress. Dilatancy, which represents an increase in porosity, was traced in the granite to open cracks which form parallel with the direction of maximum compression.

INTRODUCTION

In the study of deformation of materials one usually focuses attention on the linear rather than on the volumetric strains. With metals deformed in the ductile range this is justified, for volume changes are typically small enough to be ignored. In the compression of a block or twisting of a hollow tube of, say, copper, changes in cross-sectional area or length may amount to a hundred times or more the change in volume, and, whereas most of the linear change is permanent, almost none of the volume change is. In fact, it is very difficult to detect permanent changes in density in ductile metals caused by deformation.

For rocks, a number of observations suggest that the situation may be quite different. Appreciable permanent volume changes, of both signs, have been noted. *Handin et al.* [1963], for example, found that the density of a sandstone and a limestone increased as they were stressed to failure in confined compression tests. Similar behavior was observed for sand [*Borg et al.*, 1960] when confining pressure was fairly high. Of course this was not surprising, for these materials all had high porosity initially (10 to 20%), and some compaction would be expected from a high effective confining pressure. The opposite effect, *dilatancy*,[2] accompanied fracture of these materials when confining pressure was very low. Again, this was not surprising, for dilatancy is a well-known characteristic of granular aggregates such as dense sand. Evidently at low pressure the limestone and sandstone responded to shearing stress much the way dense sand did, that is, by sliding along rough intergranular surfaces [*Handin et al.*, 1963].

Scattered observations suggest that these are not the only geologic materials which are di-

[1] Formerly with U. S. Geological Survey.

[2] We will use the term 'dilatancy' to mean the increase of volume relative to elastic changes, caused by deformation. We follow *Mead* [1925] and use the term for any sort of solid, not just 'granular masses,' as in the original usage [*Reynolds*, 1901].

latant. *Bridgman* [1949] found that two dense, rather ductile rocks, soapstone and calcite marble, became dilatant at fracture at room pressure, and *Handin et al.* [1963] showed that a coarse-grained dolomite was dilatant even under confining pressure of several kilobars. *Robertson* [1960] found that marble deformed at several kilobars pressure increased in volume by as much as 2%.

Among the brittle rocks, *Bridgman* [1949] found very slight volume increase for a diabase and *Matsushima* [1960*b*] reported a small but pronounced increase relative to elastic volume changes for a granite and a quartz monzonite, as they were fractured in compression.

Taken together, these observations suggest that the porosity of many rocks, particularly those with initially very low porosity, increases slightly during deformation, even under confining pressure. If this is generally true, it may have widespread significance. For one thing, if rocks are generally dilatant during fracture, this will have to be taken into account in a general fracture theory, particularly one which predicts how strength depends on pressure. At present, none of the existing theories, such as those of Mohr or Griffith, is based on a model which increases in volume as it deforms. For another thing, dilatancy leads, under certain circumstances, to changes in pore pressure, and, if dilatancy is a fairly general phenomenon, we might expect widespread effects, such as those discussed by *Mead* [1925] and *Frank* [1965].

Although the above observations suggested a fairly general phenomenon, it seemed worth while to explore the matter further. For one thing, it was not clear to what extent the confining pressure would suppress dilatancy. Also, there was a possibility that part of the observed dilatancy, particularly of brittle rocks, might be due to the vertical splitting which often accompanies compressive failure (see Plate 1, *Griggs* [1936], for example). This matter could be resolved, either by the use of dogbone-shaped specimens or by carrying out the experiment under high confining pressure; vertical splitting disappears in either case [*Brace,* 1964*b*]. And, finally, it was of some interest to determine how the magnitude of volume change at fracture varies with the stress state. Is there a 'critical void ratio' [*Scott,* 1963, p. 310] at fracture for a particular rock? A number of experiments were carried out with these questions in mind.

Experimental Procedure

Volumetric strains that accompany deformation have been measured in two ways. *Bridgman* [1949] immersed a sample in a fluid-filled container and followed changes in the fluid level. *Handin et al.* [1963] observed changes in pore volume of a rock specimen. Both methods had the disadvantage of low sensitivity but the advantage of being a direct measurement of volume change. In addition, they still gave accurate results even if deformation of the sample was inhomogeneous.

The method used here depends on measurement of the principal linear strains. The part of the specimen where the measurements were made had a cylindrical shape, so that the principal strains were the axial strain ϵ_z and the circumferential strain ϵ_θ. Strain gages were used to measure strain; the axial gages had various lengths, and the circumferential gages extended to very nearly half of the full circumference. Then, as long as the circular cross section of the specimen remained circular or became elliptical during the deformation, volume change, $\Delta V/V_0$, of the specimen was

$$\Delta V/V_0 = \epsilon_z + 2\epsilon_\theta \qquad (1)$$

The present method had the advantage of high sensitivity; volume changes of 10^{-5} were readily detectable. However, it also suffered from a disadvantage. Faulting is a highly localized deformation, and (1) could hardly be expected to hold once individual fractures formed. Therefore, the volumetric strains calculated from the linear strains just before fracture of the rocks were not accurate.

Compression tests. Dogbone-shaped specimens were used for the compression tests [*Brace,* 1964*b*] to avoid end effects and to eliminate vertical splitting, insofar as this might be due to end effects. Three-dimensional photoelastic analysis of this specimen shape has recently shown [*Hoek,* 1965] that stress concentrations are negligible in the central cylindrical section and that the stresses there are very nearly uniform.

Electric resistance strain gages were mounted, as described elsewhere [*Brace,* 1964*a*], in the center section of the specimens. The jacketing

material which covered gages and center section was room-temperature vulcanizing rubber (General Electric RTV 102).

The experimental technique is the same as described in an earlier study [*Brace,* 1964*b*] with a few modifications. A constant loading rate of about 10 bars/sec was achieved by use of a Vanguard electric hydraulic pump, the output of which was metered by a HPH pressure control valve.

The loading machine used in the previous tests had a rather low spring constant (0.6 to 1.0×10^{11} dynes/cm). Inasmuch as the samples had a spring constant of 1.0×10^{11} dynes/cm or more, intrinsic behavior of the rock could not be observed once the load-deformation curve began to fall. To improve this situation, which was particularly troublesome in tests at room pressure, a stiffening element [*Paulding,* 1965] was incorporated into the loading machine. This consisted of a very stiff, simple supported beam which was so placed that it carried a major part of the load imposed by the machine on the specimen. This was equivalent to placing a stiff spring *in parallel* with the specimen. In this way the spring constant of the machine was raised to about 10 times that of the rock specimen. With this arrangement, collapse of the specimen at fracture was not nearly as sudden, and a number of stress-strain curves were obtained at room pressure which showed a distinct maximum. The stiffening element was not used in the confined compression tests. An extra 'stiffening' of the machine under these conditions is provided by friction at the high-pressure seals and by the compression of the confining medium when the sample starts to fail.

Rocks studied. With the objectives given above, three rocks were chosen for study. One, a medium-grained calcite marble, was very ductile even at low confining pressure. The two other rocks were brittle at all pressures attained. One of these, a quartz-oligoclase aplite was fine-grained and flinty and had extremely high strength. The other was Westerly granite; the strength of this rock was low enough so that behavior could be studied over a wide range of pressure. The granite had appreciable crack porosity [*Brace,* 1965], whereas the aplite had essentially none.

The particular sample of Westerly granite has been described before [*Brace,* 1964*b*, 1965]. The axial direction of the specimens here was the 1-direction of the previous studies. The calcite marble, of unknown source, was nearly pure calcite and appeared isotropic. Grain size was about 0.2 mm. The aplite occurs in the mines of the central Witwatersrand of South Africa and is known locally as 'chert dyke.' It contains about 63% oligoclase, 27% quartz, and 10% biotite. The feldspar is highly altered. Density is 2.614 g/cm^3; grain size of the ground mass is about 0.040 mm and of the phenocrysts about 0.10 mm. The rock appears isotropic.

Observations

Tests at atmospheric pressure. Stress-strain curves are shown in Figure 1*a* for compression of Westerly granite at atmospheric pressure. The compressive strength C at atmospheric pressure had previously been found to be 2.3 ± 0.1 kb, and, in this test, about 95% of this stress was applied and then removed, giving the curves shown. C is the value of the axial stress $-\sigma_z$ at fracture.

In this experiment, $-\sigma_z$ was increased at a rate of about 100 bars/sec up to about half the fracture stress, at which the rock began to creep noticeably. Load was then held constant for several minutes at increments of stress of a few hundred bars, giving the steps in the two curves. These steps became broader as stress was increased. Finally, while the rock was still intact, $-\sigma_z$ was reduced, again in increments of a few hundred bars. This time the rock did not creep, as it did on the ascending loop. As the stress reached zero, the rock had a permanent circumferential strain but little or no permanent axial strain.

Values along the two stress–linear strain curves were used in calculating volume change according to (1), giving a curve of stress–volumetric strain. The ratio $-\epsilon_\theta/\epsilon_z$ for the ascending loop is also shown in Figure 1*a*.

With increasing stress, volume first decreased (sharply at first and then nearly linearly), reached a minimum, and, finally, increased. When stress was removed, a positive volumetric strain, P, remained.

By analogy with measurements of linear compressibility, the part of the ascending stress–volumetric strain curve up to the end of the near-linear region represents elastic behavior. At least, if stress was cycled within this region,

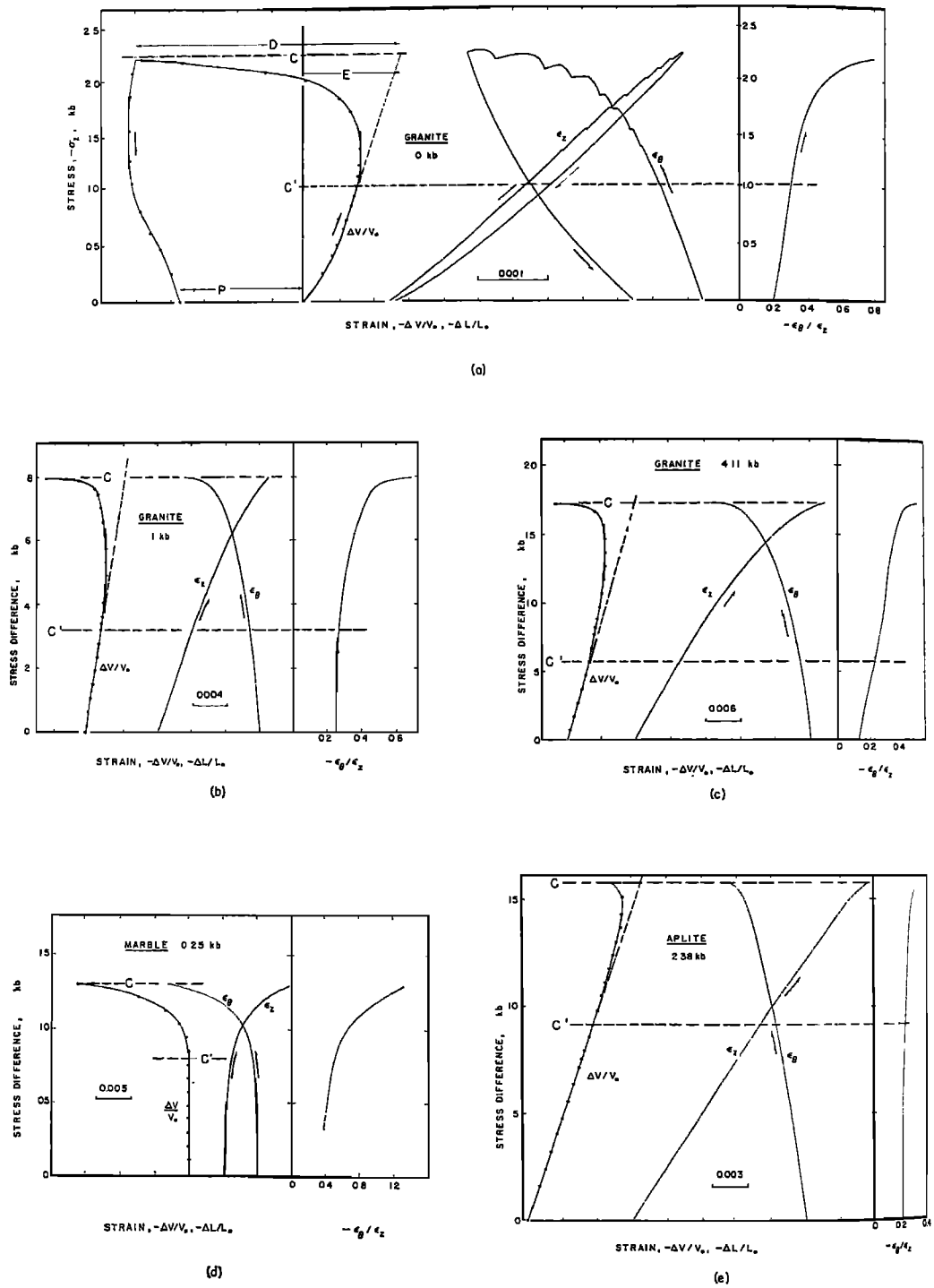

Fig. 1. Stress-strain relations. Left-hand curve, which shows stress versus volumetric strain, was calculated from the curves of stress versus axial and stress versus circumferential strain, which are tracings of XY-recorder records made during the experiments. Symbols are explained in the text.

no permanent linear or volumetric strain remained. A measure of the elastic strain the specimen should have at fracture is given by extending this linear part of the stress–volumetric strain curve up to the fracture stress C. The volumetric strain at this stress is called E. The axial stress at which the stress–volumetric strain leaves the linear region, called C', can be located approximately. For this specimen it was 1.1 ± 0.1 kb, or about $C/2$. The maximum departure of the stress–volumetric strain curve from the line representing elastic behavior, which is a net volume increase, is called D.

Values of C, C', D, and E for the granite, marble, and aplite are collected in Table 1. The uncertainty in C is a few per cent, in C' 10 to 15%, and in E about 10%. As noted above, D is a very rough measure of the total dilation at fracture, with an uncertainty of at least a factor of 2.

Tests under confining pressure. Tests were made at pressures of up to 8 kb. Typical results for the three rocks are shown in Figures 1*b*, *c*, *d*, and *e*. The curves of stress–linear strain were traced directly from XY-recorder records; then, using (1), volumetric strain was calculated from

TABLE 1. Failure Conditions of Granite, Marble, and Aplite

C is stress difference, F and S refer to fast- or slow-loading rates, f and i to fractured and intact, respectively. For other symbols see text and Figure 1.

Rock	Loading Rate	Final Form	Pressure, kb	C', kb	C, kb	C'/C	D 10^{-3}	E 10^{-3}	D/E
Granite	F	f	0	1.3	2.27	0.55	4.5	1.75	2.6
	F	i	0	0.9	2.18	0.40	4.1	1.77	2.3
	F	i	0	1.2	2.28	0.50	3.5	1.45	2.4
(Figure 1*a*)	F	i	0	1.1	2.28	0.50	3.9	1.40	2.8
	S	f	0.50	1.4	4.39	0.30	1.4	3.0	0.5
	F	i	0.50	2.2	6.30	0.35	13.4	3.5	3.8
	S	f	0.51	1.5	4.26	0.35	1.9	2.4	0.8
(Figure 1*b*)	F	i	1.00	3.3	8.05	0.40	9.0	4.4	2.0
	F	i	1.00	3.9	9.28	0.40	9.8	4.8	2.0
	F	i	1.50	5.2	10.5	0.50	4.0	5.7	0.7
	F	i	1.50	5.2	10.6	0.50	*		
	F	f	1.62	5.0	10.7	0.45	10.4	7.2	1.4
	F	i	2.0	6.25	†				
	F	i	2.0	6.5	11.8	0.55	24.2	6.6	3.7
	S	f	2.34	3.8	10.5	0.35	*		
	S	f	3.06	4.7	14.5	0.30	15.7	8.0	2.0
	S	f	4.00	6.0	16.1	0.35	7.8	9.0	0.9
(Figure 1*c*)	S	f	4.11	5.6	17.2	0.35	13.8	12.0	1.2
	S	f	5.10	8.3	17.5	0.45	6.2	10.2	0.6
	S	f	5.30	9.7	18.6	0.50	4.7	12.8	0.4
	S	f	6.50	11.7	19.5	0.60	3.9	13.5	0.3
	S	f	8.00	13.3	22.2	0.60	4.6	10.9	0.4
Marble	S	f	0	0.2	0.46	0.45	>4.5	1.3	>3.5
(Figure 1*d*)	S	f	0.25	0.9	1.30	0.65	16	2.0	8
	S	f	0.49	1.3	2.60	0.50	>6	3.0	>2.0
Aplite	S	f	0	2.6	6.05	0.45	1.4	3.8	0.4
	S	f	0	2.8	5.95	0.45	1.0	4.0	0.3
	S	f	0.77	4.5	7.2	0.63	0.6	4.7	0.1
	S	f	0.81	5.4	7.5	0.72	0.1	4.3	0.02
	S	f	1.43	5.4	13.8	0.40	0.4	6.8	0.1
(Figure 1*e*)	S	f	2.38	9.4	15.3	0.61	2.5	13.5	0.2
	S	f	2.83	10	19.8	0.50	2.6	12.0	0.2
	S	f	3.20	14	20.7	0.68	0.9	17.0	0.1

* A fault formed directly under strain gage and destroyed it before the rock failed; hence maximum strain could not be measured.

† Pressure vessel leaked and experiment had to be terminated before fracture.

these linear strains at closely spaced intervals. A smooth curve of stress–volumetric strain was drawn through the calculated points. A plot of the ratio of linear strains versus stress is also shown.

Pressure is known to about 25 bars and the stresses to about 5%. C and C' are stress differences, that is, total axial compressive stress σ_z minus pressure.

Experiments were conducted at two loading rates. For the sample shown in Figure 1*b*, the high rate (100 bars/sec) was applied; load was held constant at intervals, as in the atmospheric pressure tests described above (the steps were omitted in tracing the curves in Figure 1*b*). For the other samples (Figures 1*c*, *d*, and *e*) load was applied at a lower rate (about 10 bars/sec). These rates have an uncertainty of about 25%.

Some of the specimens were fractured; others were recovered intact when the stress-strain curves appeared to level off. The stress at this point was probably within a few per cent of the fracture stress.

The principal new feature of the tests done under confining pressure is the disappearance of the curved toe of the stress-strain curves. This again is in accordance with general elastic behavior of rocks under pressure.

The permanent strains of the marble were so large that elastic changes could not be measured with any accuracy. (In the table, E was calculated by using the mean linear compressibility of Danby marble from *Brace* [1965]).

Measurements of linear compressibility. *Walsh* [1965*b*] and *Brace* [1965] showed that porosity in the form of cracks in rocks could be found rather accurately from observation of linear compressibility in three directions. This method was used here to see whether permanent volume changes, such as P in Figure 1, could be accounted for as cracks, and, furthermore, to determine the orientation of any newly formed cracks.

If a rock is compressed under hydrostatic pressure, linear strain is related to pressure as shown in Figure 2, for example. The upper part of the curves is nearly linear, whereas the lower part is strongly curved. In the lower part, cracks are being closed by the pressure; when the curve becomes linear, all cracks have been closed. To obtain the volume associated with

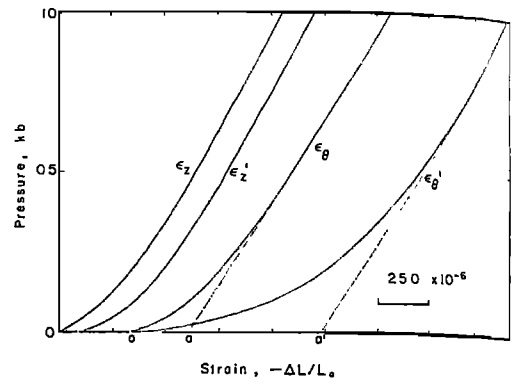

Fig. 2. Linear compressibilities of granite. Curves are tracings made from XY-recorder records showing the relation between confining pressure and strain in axial (ϵ_z) and circumferential (ϵ_θ) directions. Primed values refer to rock which has been stressed to within about 20% of the breaking stress, and unprimed values refer to virgin rock.

these cracks when open pressure–linear strain curves are needed for three perpendicular directions. In each curve an intercept oa is found (Figure 2) by projecting the linear part of the curve back to the strain axis. The sum of the intercepts for the three directions gives the volume of the rock at atmospheric pressure occupied by open cracks. The curves in Figure 2 still have slight curvatures at the top, so that the volume obtained in this way is somewhat less than the true value.

One sample of Westerly granite was stressed in compression to a stress well under C. Both linear strains were measured, and permanent change of volume noted. Linear compressibilities of the sample were next measured, using the same strain gages and the technique described in a previous study [*Brace*, 1965]. Crack porosity was calculated. Next, the sample was stressed to a somewhat higher level, new volume changes were noted, and then the linear compressibilities were remeasured. This was repeated at successively higher stresses, through C' to just under C. The results are given in Table 2; the curves of pressure–linear strain for the next to the last cycle are given in Figure 2.

In Table 2, $-\sigma_z$ is the maximum stress imposed during the particular cycle and c' is the point of departure of the stress–volume change curve from linearity *during that cycle; p* is the permanent volume increase remaining after each

TABLE 2. Cyclic Tests on Westerly Granite at Atmospheric Pressure

Cycle	$-\sigma_3$, kb	c', kb	Crack Porosity, 10^{-6} Axial ϵ_z	Circ. ϵ_θ	Total $\epsilon_z + 2\epsilon_\theta$	Total − 1580	p 10^{-6}
0			400	590	1580	0	
1	0.69		400	580	1560	−20	50
2	1.03		420	600	1620	40	100
3	1.38	1.0	430	640	1710	130	160
4	1.72	1.3	430	810	2050	470	370
5	2.11	1.6	450	1160	2770	1190	1200

cycle when stress was removed. Intercepts from pressure-linear strain curves are shown for the axial and circumferential directions together with the total, which is the axial plus twice the circumferential. This total contains for, say, the next to the last cycle, not only any newly formed cracks but also cracks present in the virgin rock. The latter must be subtracted; for the circumferential direction (Figure 2) this amounts to subtracting oa from oa'. In Table 2 this is done by subtracting initial crack porosity, 1580×10^{-6}, from the total at each cycle. The last two columns in the table contain permanent volumetric strain caused by uniaxial compression and the volume of the rock at the end of each cycle which is associated with cracks. The uncertainty in these two numbers is about 20%; sensitivity is about 50×10^{-6}.

Discussion

The stress–volumetric strain behavior of the three rocks studied has certain general characteristics. Initially, behavior is elastic. The linear part of the curve has a reciprocal slope close to the linear compressibility of the rock; they should be identical for perfect elasticity. For example, the reciprocal slope for the granite at 4.11 kb (Figure 1*c*) is 0.69 mb^{-1}; measured values of linear compressibility for this rock (extrapolated from values at 3 and 5 kb in *Brace* [1965]) are 0.68, 0.68 and 0.67 mb^{-1}, for three perpendicular directions. For the aplite (Figure 1*e*) the inverse slope is 0.62 mb^{-1}; measured linear compressibility of this rock in the axial direction of the specimens is 0.62 mb^{-1} at a pressure of 2.4 kb.

At the stress C', which is the end of the linear region and the point at which nonelastic behavior begins, volume begins to increase relative to elastic changes. When granite was stressed to a value higher than C' (about 1.0 kb) a permanent increase in volume p was detected (Table 2). As stress was increased up to the fracture stress C, the rock expanded more and more relative to the elastic changes, until it reached the maximum D just as fracture occurred.

The values C and C' for the granite are plotted in Figure 3 in the form of principal stresses. σ_3 is the maximum and σ_1 the minimum compression. Data from several other studies are added. These include tests using the large dogbone-shaped specimens described in *Brace* [1964*b*] on a new sample design described by *Mogi* [1966]. With one or two exceptions the stresses at fracture lie quite close to a smooth curve; the scatter at any one pressure is about 5%. Stresses at fracture from fast and slow tests show no consistent differences; both seem to group about the same average curve. This is in line with the rather small effect of loading rate on strength reported elsewhere for silicate rocks [*Serdengecti and Boozer*, 1961; *Matsushima*, 1960*b*].

The stresses corresponding to C' appear to be strongly time-dependent (Figure 3); all the points for the fast-loading rate fall along one line, and those from the slower tests group around another line. This grouping is shown in another way: the values of the ratio C'/C are close to 0.35 for the slow loading rate (Table 1) and close to 0.45 for the fast loading rate. There is no distinct change in this ratio with pressure for the three rocks.

In contrast to the nearly constant ratio C'/C at a given loading rate, the quantity D varies

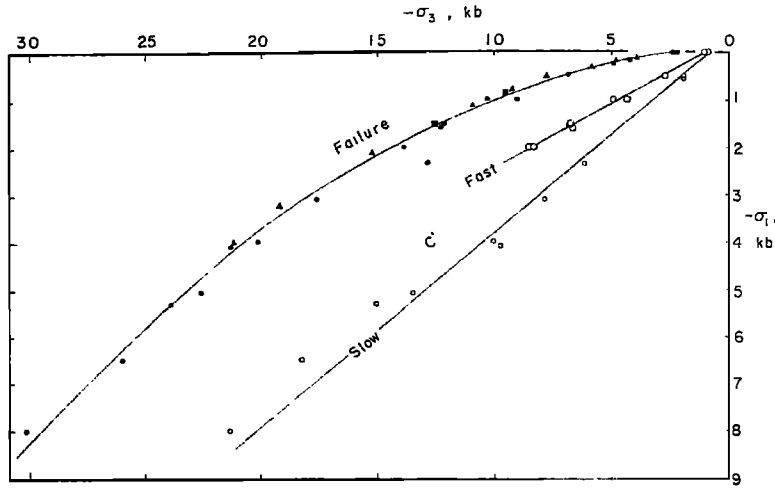

Fig. 3. Principal stresses at failure for granite. The solid points are stresses at failure, the open circles stresses at the onset of crack growth. Circles refer to present results, triangles to tests made on small dogbone-shaped specimens of a new design [*Mogi*, 1966], and squares to tests made on dogbone-shaped specimens described by *Brace* [1964*b*]. *Fast* and *slow* refer to loading rates; fast is about 100 bars/sec and slow about 10 bars/sec.

widely, even for tests at the same pressure, and even when normalized with respect to elastic volume changes (the ratio D/E in Table 1). Additional work needs to be done to determine whether this is a real feature of rocks or whether it is due solely to local inhomogeneity of the linear strains. In any event, the range of D seems to be about the same at low and at high pressure; there is no marked tendency for D to decrease with pressure. D/E is highest for marble, the most ductile rock, and lowest for the aplite.

If we may extrapolate beyond present results, the amount of dilatancy may eventually decrease. The curves for the onset of cracking (Figure 3) would appear to intersect the curve for failure at pressures beyond those attained here. Beyond this intersection we might expect no dilatancy to accompany failure.

Other measurements of volume change. Other measurements of volume change *during deformation* of nonporous rocks and of concrete are collected in Table 3 for comparison with present results. *Robertson's* [1955, 1960] measurements of *permanent* volume change for Solenhofen limestone and two marbles are collected in Table 4.

The ratio C'/C ranges from 0.35 to 0.60 and thus appears to be similar to the values found here. With the exception of the carbonate rocks, the ratio D/E has about the same range as for the present materials, although the methods of measuring volume changes varied widely. Bridgman's values of D are probably small because his samples were unjacketed. The quartzite and the diabase specimens were dogbone-shaped as in the present study, but because the strain gages were too small to give a correct average of ϵ_θ, the calculated values of D given in Table 3 may be on either side of the true one. For concrete, the volume changes shown contain an additional factor; the material compacts under pressure, so that D is reduced somewhat. This effect may become large for fairly porous rocks, as shown by *Handin et al.* [1963]. The uncertainty in the values of D given by Matsushima is quite large, as the length of strain gage used in the linear strain measurement was not reported. The values shown may be larger or smaller than the true value. Also, some of the materials in Table 3 were recovered intact, so that the value of D given is at best a lower limit. The volume changes given in Table 4, although of the same sign as the present results, are somewhat higher. This may indeed be a characteristic of carbonate rocks; the marble studied here (Table 1) had a larger D than the silicate rocks. However,

TABLE 3. Volume Changes in Crystalline Rocks and Concrete
See Table 1 for symbols.

Material	Pressure, kb	C, kb	C'/C	D 10^{-3}	D/E	Remarks
Dolomite rock	0.25	5.3		36		[*Handin et al.*, 1963] D includes elastic changes and is the value at e_z = 0.14. Initial porosity was in the form of cracks and was about 0.035.
	0.50	5.4		27		
	1.0	5.6		25		
	1.5	5.9		16		
Calcite marble	0	0.51	0.6	1.0	2.1	[*Bridgman*, 1949] Sample recovered intact.
Soapstone	0	0.65	0.6	0.4	0.6	[*Bridgman*, 1949] Sample fractured.
Diabase	0	2.3	0.6	0.4	0.1	[*Bridgman*, 1949] Sample fractured.
Quartz monzonite	0	2.0	0.6	2.0	2.3	[*Matsushima*, 1960*b*] Sample fractured.
Olivine basalt	0	1.5	0.5	3.0	1.5	[*Matsushima*, 1960*b*] Sample fractured.
Granite	0.55	4.9	0.4	0.5	0.2	[*Matsushima*, 1960*c*] Sample fractured.
	1.02	6.7	0.5	3.0	0.6	[*Matsushima*, 1960*c*] Sample fractured.
	1.50	9.1	0.4	1.0	0.2	[*Matsushima*, 1960*c*] Sample fractured.
	2.60	10.4	0.6	1.0	0.3	[*Matsushima*, 1960*c*] Sample fractured.
	3.20	12.1	0.5	1.5	0.2	[*Matsushima*, 1960*c*] Sample fractured.
	3.80	13.5	0.5	3.0	0.3	[*Matsushima*, 1960*c*] Sample fractured.
	4.40	12.1	0.5	3.0	0.5	[*Matsushima*, 1960*c*] Sample fractured.
Quartzite	0	4.61	0.5	1.0	0.2	[*Brace*, unpublished] Sample fractured.
	0.60	11.2	0.5	2.0	0.2	[*Brace*, unpublished] Sample fractured.
Diabase	0	5.15	0.6	1.9	0.8	[*Brace*, unpublished] Sample fractured.
Concrete, 1:2.1:2.5	0	0.13	0.5	0.78	1.8	[*Richart et al.*, 1929] Values given when samples were badly cracked but still intact. Confining 'pressure' applied by spiral reinforcing.
	0	0.15	0.5	1.0	2.0	
	0	0.14	0.4	1.2	2.4	
	0.010	0.19	0.6	1.7	2.4	
	0.022	0.25	0.5	1.7	1.4	
	0.027	0.25	0.4	1.3	0.9	
	0.036	0.30	0.4	2.5	1.7	

part of the difference may be due to effects associated with unloading [*Paterson*, 1963]; anomalous length changes accompany the removal of pressure in confined compression experiments with limestone. The measurements of volume change given in Table 4, having been made after pressure was removed, are not strictly comparable with those in Tables 1 and 3.

In spite of these uncertainties, two conclusions can be drawn from the present work and from results gathered from the literature (Table 3). First, with a few exceptions, fracture is accompanied by an increase in porosity which varies from 0.2 to 2 times the elastic volume decrease the material would have had were it perfectly elastic. This is apparently true for brittle as well as ductile rocks, for rocks which are loose as well as compact [*Brace*, 1964*b*, 1965], and for fracture at atmospheric pressure as well as under confining pressure of up

TABLE 4. Permanent Volume Changes in Limestone and Marble

Elastic volume changes, E, calculated assuming linear compressibility of Solenhofen limestone to be 0.82 mb^{-1} and of the marbles to be 0.44 mb^{-1}. Data from *Robertson* [1955, 1960].

Material	Pressure, kb	$-(\epsilon_z)_{max}$	C, kb	$+\Delta V/V_0$	$+(\Delta V/V_0)/E$
Solenhofen limestone	0.29	0.047	3.6	0.047	16
	0.35	0.150	3.6	0.123	41
	0.57	0.51	3.8	0.223	72
	0.75	0.16	3.8	0.089	29
	1.00	0.196	4.2	0.112	32
	2.00	0.313	5.2	0.107	25
	3.00	0.114	6.1	0.020	4
	4.00	0.217	6.7	0.043	8
Danby marble	2.50	0.097	2.5	0.010	9
	4.00	0.134	2.9	0.021	16
Rutland marble	3.00	0.073	2.3	0.004	4
	4.00	0.029	3.0	−0.004	3

to 5 kb. Second, this dilation begins at a stress one-third to two-thirds of the fracture stress. The particular ratio seems, from the present results for granite, to be strongly time-dependent—the lower the loading rate the lower the stress at which nonelastic changes commence.

It would be of some interest to explore both these effects in more detail. The existence of a critical void ratio at fracture can neither be proved nor disproved by the present results. Perhaps one of the more direct methods of measurement of D, such as was used by Handin et al. or Bridgman, might yield sufficiently accurate values of D to test such a possibility. The extent of dependence of C' on loading rate also is of considerable interest and needs to be more carefully studied. C' may also turn out to be influenced by environment; this is suggested by stress-strain curves given by *Boozer et al.* [1963].

Physical character of the volume changes. It has been known for some time that fracture in uniaxial compression, particularly of concrete, is preceded by cracking which starts at about half the fracture stress. This was detected by ultrasonic techniques [*Jones,* 1952], by special optical methods [*Berg,* 1950], by strain gages [*Blakey and Beresford,* 1955], and by direct observation of sectioned material [*Hsu et al.,* 1963]. It was of interest to see whether the increase in porosity which we had observed could be traced to cracking. One way of testing this possibility was by study of the linear compressibility of our specimens.

As noted above, linear compressibility changes when a material becomes cracked. Furthermore, if the cracking is in one direction, linear compressibility corresponding to that direction will be most strongly affected. Using the method suggested by *Walsh* [1965*b*], we can measure the porosity associated with new cracks, the *crack porosity.*

The results of this analysis for one sample of Westerly granite are given in Table 2. As compressive stress was increased, initial linear compressibility in the circumferential direction began to change markedly (Figure 2), whereas the value in the axial direction was relatively unaffected. Changes began at a stress of 1 kb, which is C' for this sample. This suggested that, beginning at C', cracks formed in the axial direction. Furthermore, the cracks that formed were open, and the crack porosity determined from linear compressibilities of the samples after stress was removed was within experimental error of the permanent increase in volume found from curves of stress–volumetric strain taken during a deformation cycle (compare last two columns of Table 2). Thus the volume changes that we had noted during deformation apparently can be traced to open axial cracks. Of course, formation of closed cracks could have preceded or accompanied this, for linear compressibility is unaffected by closed cracks.

Formation of open axial cracks at a fraction

of the maximum stress is also suggested indirectly by variation of compressional wave velocity in axial and radial directions as a function of stress. Observations for rocks [*Tocher*, 1957; *Matsushima*, 1960*a*] and for concrete [*Jones*, 1952] are all quite similar; velocity in the axial direction is hardly changed by stress, whereas velocity in a radial direction begins to decrease at about half the fracture stress. It may drop 10 to 20%.

The actual formation of cracks during deformation is very difficult to observe. Nevertheless, it seems worth while to consider the form which new cracks might have, and the ways in which they might originate. Three possible forms are shown in Figure 4.

The simplest possibility (Figure 4*a*) is the isolated axial crack; it might form along cleavages within grains or at grain boundaries. Open axial cracks might also form at the junctions of three grain boundaries or three pre-existing cracks, two of which are inclined and one is axial (Figure 4*b*). Under axial compression, sliding on the two inclined surfaces is accommodated by opening of the axial crack. By still a third possibility (Figure 4*c*), which is not unrelated to the second, axial cracks might form at either end of a pre-existing crack or grain boundary which is inclined to the axis. Axial cracks have been shown to form in this way [*Brace and Bombolakis*, 1963; *Hoek and Bieniawski*, 1966] in plastics and glass. In rocks, the new axial cracks might form along a suitably oriented grain boundary or within a grain.

Several observations suggest that the first of these possibilities is unlikely. Isolated axial cracks ought to open and close completely, with no hysteresis. Hysteresis in stress-strain curves is pronounced [*Paulding*, 1965], however, and permanent changes in volume are detected even at small stresses (Table 2). In addition, the axial strains at fracture depart from purely elastic behavior (Figures 1*a* through *e*) by an appreciable amount. This would not occur if all new cracks were simply isolated axial cracks.

Either the second or the third mechanism shown in Figure 4 seems likely. Unfortunately, microscope techniques are as yet inadequate to prove which actually does occur. But either mechanism would give hysteresis during a cycle of increasing and decreasing stress and either mechanism might show an apparent permanent

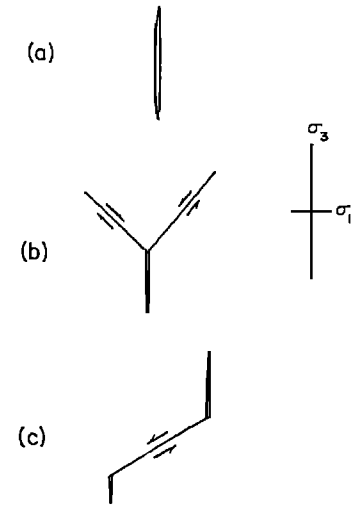

Fig. 4. Crack geometry. Three types of open axial crack are given with reference to principal stress directions.

strain, in the manner suggested by *Walsh* [1965*a*, *b*] in his analysis of elastic behavior of rocks under uniaxial stress.

Stages in the brittle fracture of rocks. From study of brittle fracture of various rocks, *Brace* [1964*b*] suggested that a typical axial stress–axial strain curve leading up to brittle fracture might consist of four parts (Figure 5*a*). Parts I and II represented elastic behavior; the existence of a recognizable toe, region I, depended on whether the rock initially contained cracks. In region III, grain boundaries supposedly loosened throughout the rock. Growth of cracks from grain boundaries and formation of faults were believed to occur in a small region of nearly constant stress, region IV. It is of interest to re-examine this scheme in the light of present findings.

In the present study, we focused attention on volumetric rather than linear strains; for comparison, a schematic axial stress–volumetric strain curve is shown, together with the linear stress–strain curve, in Figure 5. Some of the results given above can be restated in relation to these stress-strain curves. Note that *stress* here refers to the stress difference σ_D in the axial direction; if σ_z is total axial stress, σ_D equals $|\sigma_z|$ minus confining pressure.

We believe, as before, that behavior is primarily elastic in regions I and II. At least, no

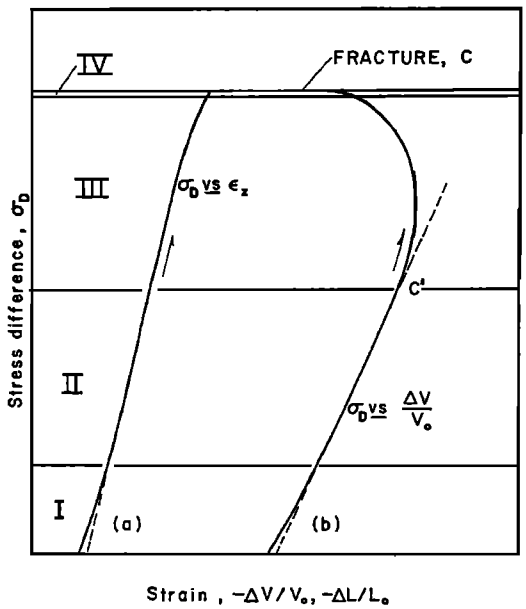

Fig. 5. Idealized stress-strain curves. (*a*) Stress versus linear (axial) strain; (*b*) stress versus volumetric strain. Behavior in each of the four regions, I, II, III, and IV, is discussed in the text.

permanent changes are observed if stress is cycled within these limits. *Walsh* [1965*a*] showed that two separate things happen in region II. First, the mineral grains distort elastically. Second, grains or parts of grains shift slightly under the applied stress and slide relative to one another. This leads to hysteresis [*Cook and Hodgson*, 1965] and other effects. *Walsh* [1965*c*] also showed that, although sliding occurs, no hysteresis should be found in a curve of stress–volumetric strain if the volumetric strain is calculated from (1). This means that such a curve portrays only the elastic distortion of the grains and, therefore, the inverse slope ought to be equal to the linear compressibility. We showed above that this was true for several compression tests under confining pressure. Through region II, then, behavior is still that of virgin rock.

The beginning of region III coincides with the point we have here called C'. As suggested in Figure 5, this point can be more easily located in a stress–volumetric strain curve than in the stress–linear strain curves, although the former is derived from the latter. In region III, elastic distortion of the grains and frictional sliding continues, along with formation of open axial cracks as described above.

Formation of open axial cracks was apparently overlooked in the earlier study, in which rocks which had been stressed to within region III were examined microscopically. There may have been several reasons for this. For one thing, new open axial cracks could not easily be detected if they were along grain boundaries. In Figure 4*a* and 4*c*, for example, both inclined and axial cracks might be at grain boundaries; since the crack walls of an open axial crack are probably no more than a few microns apart, both axial and inclined cracks would appear equally 'detached' in a polished section. Another source of this discrepancy may have been the sectioning procedure used in the earlier study. It is almost impossible not to introduce cracks during sectioning of a rock. Cracks from this source would probably be randomly oriented, and this might obscure a pattern of cracking due to stress.

Formation of open axial cracks near the ends of closed inclined cracks along which sliding occurs (which we postulate occurs in region III) suggests behavior similar to that observed in some simpler systems. *Brace and Bombolakis* [1963] and *Hoek and Bieniawski* [1966] studied crack growth photoelastically. Inclined cracks were cut in glass and plastic specimens, which were then loaded to failure in uniaxial or biaxial compression. Two features characterized all of the experiments: new crack growth was in an axial direction, and initial crack growth did not lead to failure. The load at failure of a specimen was often many times that required to initiate cracking. This behavior is qualitatively the same as what we have observed here. Both the rocks and the glass and plastic specimens illustrate an interesting aspect of failure in compression, namely, that crack growth in compression does not immediately produce a mechanical instability as it does in tension. Cracks grow and then become stable, giving an effect which might be called *crack hardening*. The rising stress-strain curve throughout region III shows that the stress required to make a crack grow actually increases after some crack growth has occurred. This is shown quantitatively for granite in Table 2; the stress to cause new cracking, here

called c', increases with each cycle to a higher stress. Although this needs to be verified by direct observation of the new cracks, the process in detail might be as follows.

From the usual arguments given in brittle fracture theory, the longest cracks will grow first. These grow and become stable, and then shorter and less favorably oriented cracks are successively activated as stress is raised. All of these grow by lengthening in an axial direction; sliding on the inclined cracks then causes the axial cracks to open. At this stage the rock is observed to be dilatant.

The exact sequence of events which characterizes region IV is still the poorest known element in the entire scheme. Evidently the crack growth of region III ultimately leads to some sort of mechanical instability. Faults rapidly form out of systems of cracks, and failure of the rock occurs. The cause of the instability is not known, nor can the rather closely reproducible failure stress be explained. But one thing is certain; formation of the final fault from the cracks of region III requires almost as much additional stress as that required to initiate crack growth.

Applicability of Griffith theory to fracture of rocks. In the previous study [*Brace*, 1964*b*], applicability of modified Griffith theory was also tested, both from the point of view of the mathematical model on which the theory is based and in terms of fracture stresses predicted by the theory. From data then available, agreement of theory and observations was good, if one accepted the possibility of rather high values of coefficients of friction (up to 1.2) at crack surfaces. In the earlier view of the fracture process, new crack growth was believed to begin in region IV. Since region IV was very small, the stress to cause crack growth, the Griffith stress, could not be very different from the fracture stress. This meant that the modified Griffith theory should predict the strength of a rock fairly closely. However, the present results have shown that crack growth begins much earlier than we had believed, at stresses much below the fracture stress. Therefore, the Griffith model really does not apply when a rock is fractured in compression. Fracture occurs by faulting; a fault may be triggered by growth of a crack, but it is almost certainly not the simple process described by Griffith theory, in which failure results from growth of the critically oriented, most highly stressed crack. In rocks, the critical 'Griffith crack' very likely grows and becomes stable at a stress near C'.

Dilatancy. Mead [1925] and more recently *Frank* [1965] have discussed some of the mechanical effects of dilatancy. Perhaps the most important of these is *dilatancy hardening*. Let us consider a porous material such as a rock, under a certain total confining pressure and, in addition, a pore pressure. The difference between these is the effective confining pressure. *Handin et al.* [1963] show that, in the presence of pore fluids, strength in compression is determined by the effective, rather than the total, confining pressure. If a rock becomes dilatant and the total volume of pore fluids is fixed, pore pressure must decrease and effective confining pressure must increase. The rock becomes stronger as a result. It is of interest to estimate the magnitude of this effect for rocks.

Under a few kilobars effective confining pressure the only pore space in a rock such as granite will be the pore porosity. For typical crystalline rocks, *Brace* [1965] and *Brace et al.* [1965] show that pore porosity ranges from about 0.001 to 0.01; for most rocks, pore porosity is nearer the lower value. The values of D from Tables 1 and 3 are of about this same magnitude. Thus the pore space will be approximately doubled in an extreme case, when rocks such as these approach failure and become dilatant. Since water expands by only about 20% when pressure is reduced by 10 kb, doubling of the pore volume would more than be sufficient to reduce pore pressure in, say, a typical crustal rock to nearly zero. This might raise strength by a considerable amount. It would be only a temporary strengthening, however, for pore fluids in adjacent unstressed rock would tend to flow into the region of reduced pore pressure.

Frank [1965] also discusses a mechanical instability which can result from dilatancy. The existence of a potential instability depends on the detailed way in which newly created pore space (D, in our terms) varies with shearing strain γ. In particular, as long as $d^2D/d\gamma^2$ is positive, the system is stable; if $d^2D/d\gamma^2$ becomes negative, the system is unstable. It is of interest to see whether the rocks studied here

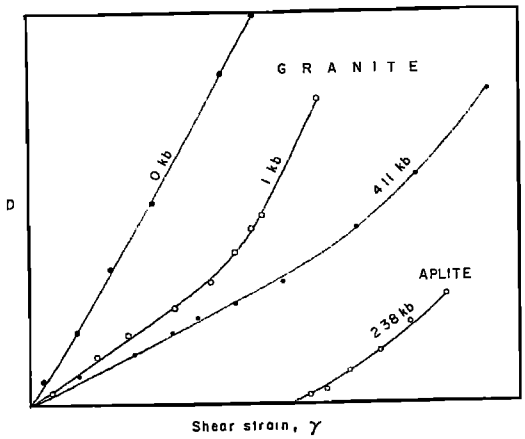

Fig. 6. Relation between newly created pore space D and shear strain γ to an arbitrary scale. The values of D and γ for these curves were taken at a number of points along the stress-strain curves in Figure 1; γ, the nonelastic part of the shear strain, is calculated as described in the text.

are potentially unstable. To do this we have to see how D and γ are related.

Plots of D versus γ are shown in Figure 6 for aplite and granite, deformed at various confining pressures. γ is assumed to be $[(e_s' - e_s') \sin 2\theta]/2$. θ is the angle of inclination of the fault to the axis, and the strains e_s' and e_s' are the residuals obtained by subtracting the elastic strains from the actual strains. The elastic strains were found by projecting the early linear parts of the curves to higher stress.

In Figure 6, slopes are positive throughout, and the second derivative is also positive, at least for large values of D. Near the origin, uncertainties in the data are large; an inflection could be present. However, we conclude that the dilatancy instability proposed by Frank would probably not develop for the kinds of rocks we have investigated. It might still be important at much lower strain rates or at high temperature.

Acknowledgments. Work by B. W. Paulding was a doctoral dissertation and was supported in part by the U. S. Geological Survey, and some of the apparatus was supplied by the Geological Survey. E. C. Robertson, J. B. Walsh, K. Mogi, and J. D. Byerlee suggested a number of improvements to the manuscript.

This work was supported by the National Science Foundation under grant GP-1470 and by the Theoretical Geophysics Branch of the U. S. Geological Survey. This help is gratefully acknowledged.

Publication authorized by the Director, U. S. Geological Survey.

References

Berg, O. Y., On the problem of strength and plasticity of concrete, *Dokl. Akad. Nauk SSSR*, *70*(4), 617–620, 1950.

Blakey, F. A., and F. D. Beresford, Tensile strains in concrete, *Australia CSIRO Div. Bldg. Res., Repts. C22-1, C22-2*, 1955.

Boozer, G. D., K. H. Hiller and S. Serdengecti, Effects of pore fluids on the deformation behavior of rocks subjected to triaxial compression in rock mechanics, edited by C. Fairhurst, pp. 579–625, Pergamon Press, New York, 1963.

Borg, I., M. Friedman, J. Handin, and D. V. Higgs, Experimental deformation of St. Peter sand: A study of cataclastic flow, *Geol. Soc. Am. Mem. 79*, pp. 133–191, 1960.

Brace, W. F., and E. G. Bombolakis, A note on brittle crack growth in compression, *J. Geophys. Res., 68*(12), 3709–3713, 1963.

Brace, W. F., Effect of pressure on electric-resistance strain gages, *Exp. Mechanics*, *4*(7), 212–216, 1964*a*.

Brace, W. F., Brittle fracture of rocks in state of stress in the earth's crust, edited by W. R. Judd, pp. 110–178, American Elsevier Publishing Company, New York, 1964*b*.

Brace, W. F., Some new measurements of linear compressibility of rocks, *J. Geophys. Res.*, *70*(2), 391–398, 1965.

Brace, W. F., A. S. Orange, and T. M. Madden, The effect of pressure on the electrical resistivity of water-saturated crystalline rocks, *J. Geophys. Res.*, *70*(22), 5669–5678, 1965.

Bridgman, P., Volume changes in the plastic stages of simple compression, *J. Appl. Phys., 20*, 1241–1251, 1949.

Cook, N. G. W., and K. Hodgson, Some detailed stress-strain curves for rock, *J. Geophys. Res.*, *70*(12), 2883–2888, 1965.

Frank, F. C., On dilatancy in relation to seismic sources, *Rev. Geophys., 3*, 484–503, 1965.

Griggs, D. T., Deformation of rocks under high confining pressures, *J. Geol., 47*, 225–251, 1936.

Handin, J., R. V. Hager, Jr., M. Friedman, and J. N. Feather, Experimental deformation of sedimentary rocks under confining pressure: Pore pressure tests, *Bull. Am. Assoc. Petrol. Geologists, 47*, 717–755, 1963.

Hoek, E., Rock fracture under static stress conditions, *S. African CSIR Rept. MEG 383*, 159 pp., Pretoria, South Africa, October, 1965.

Hoek, E., and Z. T. Bieniawski, Brittle fracture propagation in compression, *Intern. J. Fracture Mech.*, in press, 1966.

Hsu, T. T. C., F. O. Slate, G. M. Sturman, and G. Winter, Microcracking of plain concrete and the shape of the stress-strain curve, *J. Am. Concrete Inst., 60*(2), 209–224, 1963.

Jones, R., A method of studying the formation of cracks in a material subjected to stress, *Brit. J. Appl. Phys., 3,* 229–232, 1952.

Matsushima, S., Variation of the elastic wave velocities of rocks in the process of deformation and fracture under high pressure, *Disaster Prevention Res. Inst., Kyoto Univ., Bull. 32,* 1–8, 1960*a*.

Matsushima, S., On the flow and fracture of igneous rocks, *Disaster Prevention Res. Inst., Kyoto Univ., Bull. 36,* 2–9, 1960*b*.

Matsushima, S., On the deformation and fracture of granite under high confining pressure, *Disaster Prevention Res. Inst., Kyoto Univ., Bull. 36,* 11–20, 1960*c*.

Mead, Warren J., The geologic role of dilatancy, *J. Geol., 33,* 685–698, 1925.

Mogi, K., Some precise measurements of fracture strength of rocks under uniform compressive stress, *Felsmech. Ingenieurgeol.,* in press, 1966.

Paterson, M. S., Secondary length changes with pressure in experimentally deformed rocks, *Proc. Roy. Soc. London, A, 271,* 57–87, 1963.

Paulding, B. W., Jr., Crack growth during brittle fracture in compression, Ph.D. thesis, 184 pp., Massachusetts Institute of Technology, June 1965.

Reynolds, Osborn, *Sci. Papers, 2,* 217, 1901.

Richart, F. E., A. Brandtzaeg, and R. L. Brown, The failure of plain and spirally reinforced concrete in compression, *Univ. Illinois Bull., Eng. Expt. Sta. Bull., 190,* 72 pp., 1929.

Robertson, E. C., Experimental study of the strength of rocks, *Bull. Geol. Soc. Am., 66,* 1275–1314, 1955.

Robertson, E. C., Creep in Solenhofen limestone, *Geol. Soc. Am. Mem. 79,* pp. 227–244, 1960.

Scott, Ronald F., Principles of soil mechanics, 550 pp., Addison Wesley, Reading, Mass., 1963.

Serdengecti, S., and G. D. Boozer, The effects of strain rate and temperature on the behavior of rocks subjected to triaxial compression, *Bull. Mineral Ind. Expt. Sta., Penn. State Univ., 76,* 83–97, 1961.

Tocher, Don, Anisotropy in rocks under simple compression, *Trans. Am. Geophys. Union, 38,* 89–94, 1957.

Walsh, J. B., The effect of cracks on the uniaxial elastic compression of rocks, *J. Geophys. Res., 70*(2), 399–411, 1965*a*.

Walsh, J. B., The effect of cracks on the compressibility of rock, *J. Geophys. Res., 70*(2), 381–389, 1965*b*.

Walsh, J. B., The effect of cracks in rocks on Poisson's ratio, *J. Geophys. Res., 70*(20), 5249–5258, 1965*c*.

(Manuscript received March 30, 1966.)